# An overview of phase chemistry and magmatic evolution in the Cretaceous flood basalt province of northern Madagascar

LEONE MELLUSO[1*], VINCENZO MORRA[1], LORENZO FEDELE[1]

[1] Dipartimento di Scienze della Terra, Università di Napoli Federico II, via Mezzocannone 8 – 80134 Napoli, Italy

ABSTRACT. — The Cretaceous flood basalts of northern Madagascar range in composition from picritic basalt to basaltic andesite with a serial affinity ranging from tholeiitic to slightly alkaline. Rare, more evolved rocks are represented by peraluminous rhyodacites and peralkaline rhyolites. The intrusive complexes have a large range of lithologies, from ultramafic (dunites, wehrlites, clinopyroxenites) to felsic (leucogabbros, syenites). We report here the chemical composition of olivine, Ca-rich and Ca-poor pyroxene, feldspar, Fe-Cr-Ti oxide, amphibole, glass and accessory phases; the significance of their variations for what concerns geothermobarometry and regional chemical correlations is also discussed.

The evolution from the least to the most evolved compositions, and from the whole rocks towards the interstitial glasses, which are thought to be low-pressure residual liquid compositions, has been modelled with fractionation of the observed phases, leaving Mg- to Fe-rich gabbroic solids.

RIASSUNTO. — Le rocce vulcaniche Cretaciche del Madagascar settentrionale variano in composizione da basalto picritico fino ad andesite basaltica, con rare rocce più evolute (riodaciti peralluminose, rioliti alcaline); l'affinità magmatica varia da tholeiitica a transizionale-alcalina. Le rocce intrusive hanno anch'esse un significativo intervallo compositivo, variando da duniti e wehrliti, fino a gabbri e sieniti. In questo lavoro sono riportate le composizioni dei principali minerali osservati (olivine, pirosseni,
feldspati, ossidi, anfiboli e fasi accessorie), nonché dei vetri interstiziali. Inoltre, sono riportate le principali deduzioni termobarometriche e le correlazioni di significato regionale. L'evoluzione magmatica dalle composizioni più primitive a quelle meno evolute e dalle rocce totali ai vetri interstiziali sono state modellate con processi di cristallizzazione frazionata delle fasi mineralogiche presenti, attraverso la sottrazione di composizione gabbrica s.l.

KEY WORDS: *mineral and glass chemistry; fractional crystallization, geothemobarometry, Madagascan flood basalt province.*

## INTRODUCTION

The Madagascar flood basalt province was emplaced in a time span from 92 to 84 Ma (Storey *et al.*, 1995; Melluso *et al.*, 2005). The products of this province crop out throughout the island, with most outcrops found in areas close to the coast. A few dyke swarms are found well within the hinterland, thus suggesting that only the areas subject to significant lithospheric thinning were the sites of eruption, whereas the center of the island (the part now dominated by the outcrops of Precambrian basement) was not involved in thinning and subsequent magmatism. Rocks coeval to those of Madagascar have been found in the southern India conjugate margin, in the form of small lava flows and dyke swarms of variable

* Corresponding author, E-mail: melluso@unina.it

composition (e.g., Anil Kumar *et al.*, 2001; L. Melluso *et al.*, in preparation).

The flood basalt province is thought to be the result of the impact of the Marion mantle plume below the Madagascan lithosphere. To date, there is no clear evidence of a chemical input of a plume component to the source of the basalts, the only clear chemical components so far identified being MORB-like mantle and continental lithosphere (both mantle and crustal portions). Evidence of magmas coming from sources that started to melt in the garnet or spinel-bearing peridotitic mantle was also given in earlier work (e.g., Storey *et al.*, 1997; Melluso *et al.*, 2003).

Petrogenetic aspects of the volcanic and plutonic sequences have been examined in a few papers (e.g., Melluso *et al.*, 2001, 2005), but a comprehensive framework about the chemical composition of the observed phases and the magmatic evolution trends for several of the known magma types is lacking in the current literature. This paper provides new data and reviews the about 800 mineral and glass compositions available from the Naples research group on the most representative chemical compositions of the northern Madagascan province.

## Magma types, geochemical affinities and petrographic features

The chemical types so far identified in central-northern Madagascar have been divided into different magma types, according to: a) serial affinity (tholeiitic or slightly alkaline), b) geochemical characteristics, and c) location of the outcrops (Figure 1; Table 1). The details have been already given in Melluso *et al.* (2003), and will be only briefly summarized here.

In the central western part of the province (Mailaka), a transitional (TR) and a tholeiitic (THO) series have been identified. The transitional rocks show a narrow chemical range (they are mostly picritic basalts and basalts), whereas the tholeiitic series ranges from picritic basalt to rhyodacite (cf. Melluso *et al.*, 2001). Chemically similar rocks have been found in the Morondava area, just south of the Mailaka-Bemaraha areas (Bardintzeff *et al.*, 2001). In the Antanimena plateau, two tholeiitic magma types have been identified: the low-Ti-

Nb rocks, which are mostly basalts and basaltic andesites with typically low contents of all high field strength elements and relatively high $SiO_2$ contents, whereas the high-Ti low-Nb rocks are evolved tholeiitic ferrobasalts and ferrobasaltic andesites ($Fe_2O_{3t}$=14.4-15.5 wt.%), but with low Nb contents (3-9 ppm). To the east of the Antanimena plateau and in the Tamatave-Sainte Marie Island-Sambava regions of the east coast, two main magma types with thoeliitic affinity have been found: the low-La/Yb and the high La/Yb basalts, different mostly for the different degree of enrichment in incompatible contents and radiogenic isotope ratios (Melluso *et al.*, 1997, 2002, 2003). The Antampombato intrusion, composed by several mafic, ultramafic and felsic lithotypes, was filled by a different type of basalts,
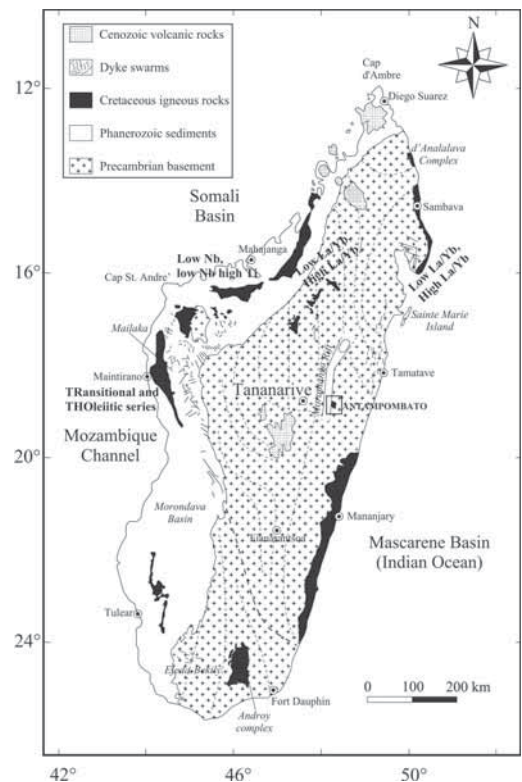


Fig. 1 – Geological map of the Madagascar, with the main outcrops of the Cretaceous igneous rocks. The position of main magma types recognized in the northern Madagascar is also located in the map.

TABLE 1 – *Whole-rock major oxide composition and chemical affinity (cf. Melluso et al., 2003) of the Madagascan rocks analysed for phase composition. Whole-rock equilibration temperatures calculated according to various geothermometers (see text) are also reported.*

| type | sample | classification | $SiO_2$ | $TiO_2$ | $Al_2O_3$ | $Fe_2O_{3t}$ | MnO | MgO | CaO | $Na_2O$ | $K_2O$ | $P_2O_5$ | LOI | T Egg | T G&J | T T&C |
|---|---|---|---|---|---|---|---|---|---|---|---|---|---|---|---|---|
| TR Mailaka | M115 | B | 45.31 | 1.57 | 13.22 | 15.19 | 0.19 | 11.75 | 9.29 | 3.16 | 0.14 | 0.19 | 0.98 | 1262 | 1082 | 1254 |
| TR Mailaka | M165 | B | 45.17 | 1.55 | 13.66 | 14.59 | 0.18 | 11.58 | 9.46 | 3.50 | 0.12 | 0.20 | 0.19 | 1258 | 1080 | 1251 |
| TR Mailaka | M111 | B | 47.22 | 1.17 | 14.49 | 13.03 | 0.18 | 9.82 | 11.53 | 2.37 | 0.05 | 0.14 | 0.39 | 1227 | 1089 | 1217 |
| TR Mailaka | M105 | B | 48.24 | 1.17 | 15.57 | 12.55 | 0.17 | 7.25 | 12.27 | 2.53 | 0.10 | 0.13 | 0.58 | 1180 | 1089 | 1168 |
| TR Mailaka | M104 | B | 47.15 | 2.54 | 16.54 | 15.42 | 0.18 | 5.59 | 8.58 | 3.64 | 0.09 | 0.27 | -0.04 | 1151 | 1078 | 1136 |
| TR Mailaka | M168 | B | 48.22 | 1.96 | 17.08 | 15.24 | 0.18 | 4.30 | 8.45 | 3.88 | 0.35 | 0.34 | -0.22 | 1127 | 1076 | 1111 |
| THO Mailaka | M162 | B | 47.68 | 0.95 | 12.20 | 14.15 | 0.19 | 13.88 | 8.42 | 1.97 | 0.37 | 0.18 | 1.71 | 1300 | 1086 | 1295 |
| THO Mailaka | M129 | B | 48.73 | 1.08 | 16.18 | 12.55 | 0.17 | 8.04 | 9.65 | 3.16 | 0.29 | 0.16 | 1.44 | 1195 | 1082 | 1183 |
| THO Mailaka | M108 | A | 56.81 | 1.30 | 14.42 | 10.30 | 0.15 | 4.79 | 8.64 | 2.52 | 0.94 | 0.12 | 1.25 | 1136 | 1080 | 1120 |
| THO Mailaka | M139 | BA | 55.57 | 1.66 | 13.41 | 13.25 | 0.18 | 4.58 | 6.78 | 3.08 | 1.25 | 0.23 | 1.41 | 1132 | 1073 | 1116 |
| THO Mailaka | M153 | A | 58.73 | 1.20 | 15.01 | 9.38 | 0.15 | 3.95 | 7.53 | 2.77 | 1.13 | 0.15 | 1.25 | 1121 | 1077 | 1104 |
| THO Mailaka | M122 | A | 56.06 | 1.69 | 13.60 | 13.51 | 0.20 | 3.09 | 6.97 | 3.40 | 1.25 | 0.23 | 1.76 | 1106 | 1072 | 1088 |
| evolved Mailaka | M145 | A | 62.65 | 1.44 | 14.14 | 8.66 | 0.15 | 2.67 | 5.37 | 3.03 | 1.76 | 0.12 | 1.23 | 1098 | 1066 | 1080 |
| evolved Mailaka | M144 | RD | 68.94 | 0.72 | 14.09 | 7.64 | 0.10 | 0.84 | 2.42 | 2.63 | 2.43 | 0.20 | 3.00 | 1065 | 1049 | 1045 |
| evolved Mailaka | M146 | RD | 69.17 | 0.71 | 14.19 | 7.52 | 0.10 | 0.69 | 2.33 | 2.73 | 2.35 | 0.21 | 2.99 | 1062 | 1048 | 1042 |
| evolved Mailaka | M148 | RD | 69.18 | 0.68 | 14.28 | 7.37 | 0.10 | 0.68 | 2.39 | 2.69 | 2.41 | 0.22 | 3.02 | 1062 | 1048 | 1042 |
| low Ti-Nb | M436 | BA | 54.02 | 1.16 | 14.82 | 11.91 | 0.22 | 4.86 | 9.23 | 3.19 | 0.43 | 0.16 | 1.66 | 1137 | 1081 | 1122 |
| low Ti-Nb | M422 | B | 46.52 | 1.25 | 13.44 | 13.38 | 0.18 | 13.17 | 9.36 | 2.40 | 0.17 | 0.15 | 3.45 | 1287 | 1086 | 1281 |
| low Ti-Nb | M78 | A | 56.18 | 1.18 | 14.54 | 10.39 | 0.18 | 4.70 | 8.45 | 3.38 | 0.81 | 0.19 | 1.54 | 1135 | 1077 | 1119 |
| low Ti-Nb | M83 | BA | 53.46 | 1.21 | 14.64 | 12.29 | 0.17 | 5.04 | 9.56 | 3.12 | 0.31 | 0.21 | 2.04 | 1141 | 1082 | 1125 |
| Low Nb high Ti | M54 | BA | 52.84 | 2.47 | 13.27 | 14.76 | 0.20 | 4.23 | 8.21 | 3.07 | 0.52 | 0.43 | 1.11 | 1126 | 1079 | 1110 |
| Low Nb high Ti | M74 | BA | 52.21 | 2.55 | 13.25 | 15.36 | 0.21 | 4.17 | 8.37 | 3.02 | 0.48 | 0.38 | n.d. | 1125 | 1079 | 1108 |
| low La/Yb | M47 | B | 50.35 | 2.28 | 14.36 | 12.90 | 0.19 | 6.31 | 10.89 | 2.27 | 0.16 | 0.28 | n.d. | 1164 | 1088 | 1150 |
| low La/Yb | M71 | B | 50.73 | 2.35 | 14.08 | 13.13 | 0.19 | 5.91 | 11.01 | 2.18 | 0.14 | 0.29 | n.d. | 1156 | 1089 | 1142 |
| Sainte Marie | SM(R) | B | 51.16 | 3.26 | 12.85 | 15.58 | 0.21 | 4.51 | 9.00 | 2.17 | 0.64 | 0.61 | 1.06 | 1131 | 1085 | 1115 |
| high La/Yb | M40 | B | 51.26 | 3.44 | 13.64 | 12.40 | 0.17 | 5.86 | 9.74 | 2.45 | 0.54 | 0.51 | n.d. | 1155 | 1085 | 1141 |
| high La/Yb | M19 | B | 51.09 | 3.85 | 13.44 | 13.64 | 0.18 | 4.63 | 9.53 | 2.84 | 0.39 | 0.41 | n.d. | 1133 | 1083 | 1117 |
| high La/Yb | M10 | B | 51.32 | 4.00 | 13.44 | 13.03 | 0.17 | 4.83 | 8.45 | 3.01 | 0.87 | 0.88 | n.d. | 1137 | 1078 | 1121 |
| high La/Yb | M7a | B | 50.67 | 3.95 | 13.45 | 12.86 | 0.16 | 6.12 | 8.32 | 2.79 | 0.87 | 0.82 | 0.61 | 1160 | 1079 | 1146 |
| high La/Yb | M6 | B | 51.95 | 4.11 | 13.70 | 12.69 | 0.16 | 4.41 | 8.50 | 2.86 | 0.73 | 0.89 | n.d. | 1129 | 1080 | 1113 |
| Tampoketsa K | M405 | B | 50.70 | 4.86 | 12.91 | 14.68 | 0.19 | 5.27 | 9.47 | 2.98 | 0.73 | 0.59 | 0.15 | 1145 | 1081 | 1130 |
| Antampombato | M497a | B | 46.86 | 2.15 | 12.40 | 14.03 | 0.21 | 9.61 | 11.46 | 2.59 | 0.43 | 0.27 | 0.04 | 1223 | 1087 | 1213 |
| Antampombato | M500 | B | 47.55 | 2.36 | 12.44 | 14.60 | 0.22 | 7.81 | 11.27 | 2.80 | 0.66 | 0.29 | 1.18 | 1191 | 1085 | 1178 |
| Antampombato | M460 | dunite | 40.68 | 0.08 | 1.00 | 15.35 | 0.22 | 41.70 | 0.92 | 0.02 | 0.01 | 0.01 | 7.99 | | | |
| Antampombato | M462 | wehrlite | 44.73 | 0.23 | 1.45 | 11.36 | 0.15 | 34.17 | 7.85 | 0.02 | 0.01 | 0.02 | 4.99 | | | |
| Antampombato | M451 | wehrlite | 41.47 | 0.71 | 1.64 | 18.05 | 0.27 | 34.49 | 3.28 | 0.07 | 0.01 | 0.01 | 1.42 | | | |
| Antampombato | M496 | gabbro | 48.63 | 1.39 | 9.44 | 10.76 | 0.17 | 13.34 | 13.97 | 1.64 | 0.44 | 0.23 | 0.67 | | | |
| Antampombato | M471 | gabbro | 46.29 | 0.46 | 15.00 | 6.38 | 0.10 | 12.63 | 17.32 | 1.80 | 0.01 | 0.01 | 0.48 | | | |
| Antampombato | M470 | gabbro | 45.62 | 2.03 | 12.59 | 12.94 | 0.19 | 11.36 | 12.74 | 1.58 | 0.77 | 0.18 | 2.56 | | | |
| Antampombato | M495 | gabbro | 47.43 | 0.99 | 5.57 | 10.45 | 0.15 | 24.36 | 9.40 | 1.27 | 0.21 | 0.18 | 0.56 | | | |
| Antampombato | M485 | gabbro | 45.47 | 1.40 | 8.43 | 11.87 | 0.17 | 17.21 | 13.06 | 1.90 | 0.34 | 0.16 | 1.98 | | | |
| Antampombato | M476 | leucogabbro | 55.52 | 2.01 | 16.79 | 8.77 | 0.31 | 3.71 | 5.59 | 5.36 | 1.05 | 0.88 | 0.76 | | | |
| Antampombato | M475 | mugearite | 61.74 | 1.39 | 15.64 | 6.00 | 0.24 | 2.75 | 3.86 | 5.86 | 1.97 | 0.55 | 0.46 | | | |
| Antampombato | M481 | syenite | 60.00 | 1.05 | 17.70 | 7.68 | 0.49 | 1.14 | 3.13 | 7.19 | 1.31 | 0.33 | 0.28 | | | |
| Antampombato | M484 | syenite | 63.37 | 0.67 | 18.38 | 4.07 | 0.34 | 0.64 | 2.01 | 8.67 | 1.68 | 0.16 | 0.24 | | | |

T Egg (°C)=18MgO+1050 (Eggins, 1993)
T (G&J) (°C)=1242-138.9(1-Mg#)-4.11TiO2-88.8(Na2O+K2O)/(Na2O+K2O+CaO) (Grove and Juster, 1989)
T T&C (°C)=19.198MgO+1028.5 (Toplis and Carroll, 1996)
B, basalt; BA, basaltic andesite; A, andesite; RD, rhyodacite

with respect to the high- and low-La/Yb basalts. This type has a MORB-like isotopic composition and is transitional-type in serial affinity (Melluso *et al.*, 2003, 2005). Information about the chemical types found in southern Madagascar can be found in Dostal *et al.* (1992), Storey *et al.* (1997) and Bardintzeff *et al.* (2001).

*Summary of the main petrographic features*

*Picritic basalts* are characterized by phenocrysts and microphenocrysts of olivine, with inclusions of Cr-spinel, and with less frequent plagioclase and/ or clinopyroxene phenocrysts, in a groundmass rich of feldspar, pyroxene and opaque oxide.

*Basalts, basaltic andesites and andesites* are nearly olivine-free rocks, with plagioclase and clinopyroxene phenocrysts; orthopyroxene is present as microphenocryst in a few samples, and pigeonite is mostly found in the groundmass. *Dacites* are aphyric rocks, with feldspar, pyroxene and oxide microlites, whereas *rhyodacites* are porphyritic rocks, with plagioclase, orthopyroxene, olivine, cordierite, opaques as phenocrysts in a glassy matrix. *Rhyolites* are quartz and feldspar-bearing rocks, with rare fresh mafic phases.

The *intrusive rocks* range in composition from dunites, through wehrlites and clinopyoxenites, to gabbros, leucogabbros and syenites.

The composition of the observed phases was obtained on ab. 45 mafic to felsic lithotypes, and in the most representative intrusive rocks, thus covering the complete range of known compositions (Table 1; Fig. 1). The complete data set is available from the authors in the form of an excel file, and is periodically updated after obtaining samples from different areas of this very large province. Analytical techniques are reported in the appendix.

## Phase chemistry

Olivine (95 analyses) is the most important phenocryst or groundmass phase of Mg-rich basalts, and is also present in the intrusive rocks (dunites, wehrlites and gabbros). The total compositional range is from $Fo_{87}$ to $Fo_6$, the least forsterite-rich compositions being found in groundmass olivines of Mailaka transitional basalt dykes. Olivine is absent in most intermediate rocks, such as the low-Ti-Nb and low-Nb, high-Ti rocks of Antanimena, in the high La/Yb basalts (excluding the Tampoketsa samples), and is rare in the low La/Yb basalts. Fe-rich olivine ($Fo_{15}$-$Fo_{12}$) have been found in the peraluminous rhyodacites of Mailaka (Table 2), coexisting with orthopyroxene, calcic plagioclase and cordierite.

The general distribution has a marked peak in the most Mg-rich compositions, as a consequence of dominant sampling of mafic products, and the highest Forsterite compositions reached indicate that these olivines grew up from relatively primitive liquids (Mg#=0.68-0.70, using a $K_d$Mg/Fe=0.33; Roeder and Emslie, 1970).

Pyroxene. The composition of the pyroxenes is given in fig. 3a and 3b and Table 3. Ca-rich clinopyroxenes (245 analyses) belong to the augite-Fe-augite and diopside-hedenbergite series. The first series has been found in the the tholeiitic series rocks, whereas the second series has been found in the transitional basalts of Mailaka, in the Antampombato mafic dykes and the associated mafic-ultramafic intrusives.

Minor element variations have surprisingly large ranges (cf. Table 3). It is worth noting that the diopside-hedenbergite clinopyroxenes of Mailaka and Antampombato are distinctly different in their minor element chemistry (fig. 3b). The Mailaka clinopyroxenes reach $TiO_2$ values as high as 4.7 wt.%, whereas the Antampombato clinopyroxenes reach a $TiO_2$ content of 2.3 wt.%. According to a $K_d$Fe/Mg=0.23 (Grove and Bryan, 1983), the

Table 2 – *Representative composition of olivine. Mg#= atomic Mg/(Mg+Fe).*

| sample | | $SiO_2$ | FeO | MnO | MgO | CaO | sum | Mg# |
|---|---|---|---|---|---|---|---|---|
| M115 | core | 39.13 | 18.03 | 0.35 | 41.96 | 0.24 | 99.7 | 0.80 |
| M115 | gm | 33.91 | 46.76 | 0.92 | 18.52 | 0.56 | 100.7 | 0.41 |
| M158 | core | 39.48 | 17.56 | 0.36 | 42.60 | 0.29 | 100.3 | 0.81 |
| M105 | gm | 30.12 | 64.36 | 1.80 | 2.28 | 1.58 | 100.1 | 0.06 |
| M168 | gm | 31.56 | 55.83 | 1.42 | 9.37 | 0.83 | 99.0 | 0.23 |
| M146 | gm | 30.29 | 62.32 | 1.23 | 5.08 | 0.03 | 99.0 | 0.12 |
| M422 | core | 40.63 | 12.68 | 0.21 | 46.75 | 0.25 | 100.5 | 0.87 |
| M405 | core | 36.89 | 30.90 | 0.42 | 32.55 | 0.23 | 101.0 | 0.65 |
| M461 | core | 40.62 | 12.68 | 0.17 | 47.39 | 0.40 | 101.3 | 0.87 |
| M471 | core | 38.15 | 20.75 | 0.25 | 41.32 | 0.05 | 100.5 | 0.78 |

gm, groundmass

maximum Mg# of the equilibrium liquids varies from 0.61 to 0.50, hence the clinopyroxenes with the highest MgO contents grew up from liquid compositions relatively more evolved than those where olivines crystallized (see above). None of the most Mg-rich clinopyroxenes shows evidence of crystallization at high pressures (according to the barometer of Nimis, 1999).

Ca-poor pyroxene (82 analyses). Pigeonite is also relatively abundant in the rocks of tholeiitic affinity. Its composition varies from $Ca_5Mg_{72}Fe_{23}$ to $Ca_9Mg_{33}Fe_{58}$. Mg-rich orthopyroxene has been found in a few basalts belonging to the high La/Yb types, whereas Fe-rich orthopyroxene has been found in the Mailaka peraluminous rhyodacites ($Ca_1Mg_{25-29}Fe_{70-74}$). The large range of compositions is typical of most flood basalt provinces (e.g., Deccan, Paraná, Antarctica). Equilibration temperatures of pigeonites (using the algorithm of Ishii, 1976) range from 1173 to 966°C. The transition from Mg-rich orthopyroxene to pigeonite in some high-La/Yb basalt samples is further example of the classical evolution of low-Ca pyroxene in tholeiitic suites.

TABLE 3 – *Representative compositions of pyroxenes. Ca, Mg, Fe are reported in mol%.*

| | Label | SiO$_2$ | TiO$_2$ | Al$_2$O$_3$ | FeO | MnO | MgO | CaO | Na$_2$O | Cr$_2$O$_3$ | sum | Ca | Fe* | Mg | Mg# |
|---|---|---|---|---|---|---|---|---|---|---|---|---|---|---|---|
| M162 | core | 53.23 | 0.47 | 1.64 | 6.68 | 0.32 | 16.66 | 20.15 | 0.32 | 0.34 | 99.5 | 41.3 | 11.2 | 47.5 | 0.81 |
| M139 | gm | 50.78 | 0.95 | 1.35 | 19.23 | 0.54 | 13.98 | 12.55 | 0.21 | | 99.6 | 26.5 | 32.5 | 41.0 | 0.56 |
| M108 | core | 52.33 | 0.70 | 2.43 | 8.89 | 0.35 | 18.69 | 15.63 | 0.23 | 0.33 | 99.3 | 32.0 | 14.8 | 53.2 | 0.78 |
| M120 | rim | 49.55 | 0.24 | 0.16 | 26.41 | 0.30 | 3.98 | 18.15 | 0.76 | | 99.6 | 40.8 | 46.8 | 12.4 | 0.21 |
| M160 | gm | 50.82 | 0.62 | 0.85 | 23.59 | 0.82 | 14.00 | 9.02 | 0.20 | | 99.9 | 19.0 | 40.1 | 41.0 | 0.51 |
| M153 | gm | 52.82 | 0.60 | 1.30 | 12.37 | 0.39 | 18.13 | 14.02 | 0.17 | | 99.8 | 28.5 | 20.2 | 51.3 | 0.72 |
| M115 | gm | 47.48 | 2.09 | 2.19 | 23.07 | 0.52 | 2.92 | 19.67 | 1.60 | | 99.5 | 46.7 | 43.7 | 9.6 | 0.18 |
| M158 | gm | 45.67 | 4.01 | 5.86 | 12.81 | 0.31 | 9.49 | 20.50 | 0.74 | | 99.4 | 46.6 | 23.3 | 30.0 | 0.56 |
| M105 | gm | 51.56 | 0.69 | 3.64 | 6.38 | 0.18 | 15.34 | 21.78 | 0.27 | | 99.8 | 45.1 | 10.6 | 44.2 | 0.81 |
| M105 | gm | 49.30 | 1.68 | 2.18 | 17.02 | 0.47 | 8.32 | 20.07 | 0.66 | | 99.7 | 44.3 | 30.1 | 25.6 | 0.46 |
| M168 | gm | 47.59 | 1.66 | 2.03 | 24.10 | 0.46 | 2.51 | 19.52 | 1.43 | | 99.3 | 46.3 | 45.5 | 8.3 | 0.15 |
| M104 | core | 46.99 | 3.82 | 4.47 | 13.66 | 0.13 | 9.28 | 20.63 | 0.84 | | 99.8 | 46.6 | 24.3 | 29.1 | 0.55 |
| M108 | gm | 55.01 | 0.21 | 0.65 | 13.16 | 0.28 | 26.35 | 3.92 | 0.08 | | 99.66 | 7.7 | 20.5 | 71.8 | 0.78 |
| M153 | gm | 51.52 | 0.38 | 0.59 | 25.53 | 0.72 | 16.59 | 4.33 | 0.16 | | 99.82 | 9.0 | 42.8 | 48.2 | 0.53 |
| M153 | core | 54.73 | 0.21 | 1.41 | 12.70 | 0.16 | 28.42 | 1.88 | 0.16 | | 99.67 | 3.7 | 19.5 | 76.8 | 0.80 |
| M146 | core | 46.35 | 0.30 | 3.08 | 41.06 | 0.64 | 8.24 | 0.27 | 0.05 | | 99.99 | 0.6 | 73.5 | 25.9 | 0.26 |
| M422 | gm | 49.70 | 1.87 | 4.70 | 8.36 | 0.20 | 13.89 | 21.12 | 0.44 | 0.53 | 100.8 | 44.8 | 14.2 | 41.0 | 0.74 |
| M78 | core | 52.86 | 0.57 | 1.49 | 10.12 | 0.27 | 16.75 | 17.29 | 0.28 | | 99.6 | 35.5 | 16.7 | 47.8 | 0.74 |
| M83 | gm | 52.44 | 0.77 | 5.23 | 17.85 | 0.40 | 10.99 | 12.98 | 1.26 | | 101.9 | 30.5 | 33.5 | 36.0 | 0.52 |
| M74 | core | 49.86 | 1.26 | 3.29 | 12.07 | 0.17 | 14.83 | 17.57 | 0.33 | | 99.4 | 36.8 | 20.0 | 43.2 | 0.68 |
| M71 | core | 53.00 | 0.65 | 1.95 | 7.13 | 0.25 | 16.84 | 19.12 | 0.43 | 0.54 | 99.9 | 39.6 | 11.9 | 48.5 | 0.80 |
| SM | core | 51.10 | 0.98 | 1.63 | 15.86 | 0.39 | 15.02 | 14.49 | 0.22 | | 99.7 | 30.1 | 26.4 | 43.5 | 0.62 |
| SM | rim | 49.56 | 0.62 | 0.81 | 25.40 | 0.56 | 6.82 | 15.89 | 0.30 | | 100.0 | 34.8 | 44.4 | 20.8 | 0.32 |
| M19 | core | 50.30 | 1.55 | 4.14 | 8.53 | 0.25 | 16.22 | 18.37 | 0.32 | | 99.7 | 38.4 | 14.3 | 47.2 | 0.77 |
| M7a | gm | 50.52 | 0.48 | 0.88 | 24.40 | 0.56 | 13.50 | 9.05 | 0.13 | | 99.5 | 19.1 | 41.2 | 39.7 | 0.49 |
| M6 | gm | 51.95 | 1.09 | 1.86 | 12.51 | 0.12 | 15.21 | 16.81 | 0.37 | | 99.9 | 35.1 | 20.6 | 44.2 | 0.68 |
| M19 | gm | 53.53 | 0.47 | 1.30 | 15.04 | 0.29 | 26.78 | 2.25 | 0.05 | | 99.7 | 4.4 | 23.3 | 72.4 | 0.76 |
| M54 | gm | 52.01 | 0.46 | 0.48 | 24.13 | 0.44 | 18.24 | 4.23 | 0.05 | | 100.0 | 8.7 | 39.3 | 52.0 | 0.57 |
| M71 | gm | 51.95 | 0.62 | 0.83 | 21.58 | 0.44 | 19.08 | 5.16 | 0.08 | | 99.7 | 10.6 | 35.2 | 54.3 | 0.61 |
| M7a | gm | 51.84 | 0.62 | 0.68 | 23.13 | 0.52 | 17.45 | 5.73 | 0.09 | | 100.1 | 11.8 | 38.1 | 50.1 | 0.57 |
| M6 | gm | 52.89 | 0.50 | 0.48 | 20.64 | 0.51 | 21.33 | 3.76 | 0.08 | | 100.2 | 7.5 | 33.1 | 59.4 | 0.64 |
| M497 | rim | 49.94 | 0.70 | 3.93 | 4.91 | 0.05 | 15.76 | 22.86 | 0.33 | 1.14 | 99.6 | 47.0 | 8.0 | 45.1 | 0.85 |
| M476 | gm | 55.37 | 0.08 | 0.62 | 10.30 | 1.34 | 12.69 | 22.00 | 0.58 | | 103.0 | 45.1 | 18.7 | 36.2 | 0.66 |
| M484 | rim | 51.83 | 0.22 | 0.56 | 17.23 | 2.32 | 10.18 | 20.02 | 0.55 | 0.02 | 102.9 | 40.5 | 30.9 | 28.6 | 0.48 |
| M481 | core | 49.11 | 0.11 | 0.11 | 35.75 | 4.52 | 9.34 | 1.45 | 0.06 | | 100.5 | 3.2 | 68.5 | 28.3 | 0.29 |

gm, groundmass

Oxides. Chrome-bearing spinel (50 analyses) is found as inclusion in olivine, and is a significant cumulus phase in the dunitic rocks exposed in the intrusive complexes (Antampombato). This phase reaches a $Cr_2O_3$ content of 44 wt.%, a Cr#=0.72 (Cr#= molar Cr/(Cr+Al)) (Table 4), and shows a very large range, from Al-rich to Cr-Fe-rich, Al-poor varieties (fig. 4; Table 4). The compositions show a typical bell-shaped pattern, with a marked compositional gap in the Al- or Fe-rich, but Cr-poor varieties.

Fe-Ti spinel (67 analyses) is ubiquitous and ranges from $Ulvöspinel_2$ to $Ulvöspinel_{92}$ ($TiO_2$ from 0.5 to 31.5 wt.%). This large range is very likely due to the subsolidus re-equilbration of the crystals, and not to the chemical affinity of the samples. MnO ranges from 0.01 to 4.29 wt.%, and $Al_2O_3$ is low (<4.2 wt.%). Ilmenite (33 analyses) has been found as the only oxide in the Mailaka peraluminous rhyodacites, and is usually found along with Ti-magnetite grains. The highest equilibration temperatures and the oxygen fugacities using two-oxide geothermobarometry are around 1150°C and $logfO_2$=-9.3 units (sample MAD71, low La/Yb basalt). Most data plot close to, or slightly below, the Quartz-Fayalite-Magnetite synthetic buffer (fig. 5). Low temperature re-equilibrated pairs, which can be easily observed in the Antampombato intrusive rocks, plot both above and below this buffer.

Feldspar. Plagioclase is the almost exclusive feldspar. The range of 220 chemical analyses is from $An_{92}$ to $An_4$, with the largest range found in the rocks of the Antampombato intrusion (Table 5). Most analyses are labradorites (fig. 6). The evolved rhyodacites of Mailaka are noted for having calcic plagioclase phenocrysts ($An_{65}$-$An_{39}$). These compositions are to be linked to the peraluminous chemistry of the host rocks. The composition of plagioclase in these rhyodacites is also decidedly low in total iron (0.3-0.01 wt.%), differently from the chemical composition of most feldspars found in non-peraluminous rocks.

Amphiboles. Amphiboles (34 analyses) have been found only in the Antampombato intrusive and hypabyssal rocks. They range in composition from kaersutite (in gabbros; $TiO_2$ up to 4.77 wt.%, Mg# 0.76-0.70) to Fe-edenite (in sodium-rich alkali syenites; $TiO_2$ 1.98 wt.%; Mg#=0.40) (Melluso *et al.*, 2005)

TABLE 4 – *Representative composition of feldspars. An, Ab, Or are reported in mol%.*

| No | | SiO$_2$ | Al$_2$O$_3$ | FeO | CaO | Na$_2$O | K$_2$O | sum | An mol% | Or | Ab |
|----|------|-------|-------|------|-------|-------|------|-------|---------|------|------|
| M139 | core | 55.04 | 27.81 | 0.82 | 10.12 | 5.49 | 0.36 | 99.6 | 49.4 | 2.1 | 48.5 |
| M122 | core | 54.48 | 28.29 | 0.86 | 10.66 | 5.24 | 0.27 | 99.8 | 52.1 | 1.6 | 46.3 |
| M115 | core | 49.91 | 31.40 | 0.63 | 14.43 | 3.31 | 0.05 | 99.7 | 70.5 | 0.3 | 29.2 |
| M158 | gm | 57.47 | 26.27 | 0.52 | 8.49 | 6.62 | 0.21 | 99.6 | 41.0 | 1.2 | 57.8 |
| M105 | core | 49.70 | 31.47 | 0.67 | 14.43 | 3.14 | 0.06 | 99.5 | 71.5 | 0.4 | 28.2 |
| M104 | gm | 65.65 | 20.88 | 0.27 | 1.89 | 10.05 | 0.86 | 99.6 | 9.0 | 4.9 | 86.2 |
| M145 | core | 51.24 | 30.62 | 0.38 | 13.43 | 3.70 | 0.20 | 99.6 | 66.0 | 1.2 | 32.9 |
| M144 | core | 53.67 | 29.40 | 0.01 | 11.70 | 4.67 | 0.37 | 99.8 | 56.8 | 2.1 | 41.0 |
| M144 | rim | 55.53 | 28.17 | 0.26 | 9.98 | 5.71 | 0.34 | 100.0 | 48.2 | 2.0 | 49.9 |
| M83 | gm | 63.59 | 21.96 | 0.67 | 3.28 | 8.69 | 1.34 | 99.5 | 15.9 | 7.7 | 76.3 |
| M83 | core | 49.87 | 31.21 | 0.92 | 14.24 | 3.13 | 0.10 | 99.5 | 71.1 | 0.6 | 28.3 |
| M78 | gm | 59.13 | 24.82 | 0.86 | 6.63 | 7.33 | 0.65 | 99.4 | 32.1 | 3.7 | 64.2 |
| M54 | gm | 54.94 | 27.86 | 0.93 | 10.20 | 5.48 | 0.27 | 99.7 | 49.9 | 1.6 | 48.5 |
| M54 | gm | 65.66 | 20.71 | 0.58 | 1.85 | 9.49 | 1.61 | 99.9 | 8.8 | 9.2 | 82.0 |
| M71 | core | 50.97 | 30.89 | 0.69 | 13.65 | 3.63 | 0.09 | 99.9 | 67.2 | 0.5 | 32.3 |
| M7a | gm | 54.33 | 27.94 | 1.11 | 10.42 | 5.23 | 0.35 | 99.4 | 51.3 | 2.1 | 46.6 |
| M6 | gm | 61.81 | 23.25 | 0.69 | 4.59 | 8.00 | 1.28 | 99.6 | 22.3 | 7.4 | 70.3 |
| M6 | core | 53.85 | 28.62 | 0.76 | 11.03 | 5.02 | 0.29 | 99.6 | 53.9 | 1.7 | 44.4 |
| M471 | rim | 45.51 | 34.62 | 0.39 | 18.89 | 1.30 | 0.07 | 100.8 | 88.6 | 0.4 | 11.0 |
| M497 | rim | 53.07 | 30.16 | 0.70 | 12.43 | 4.88 | 0.15 | 101.4 | 58.0 | 0.8 | 41.2 |
| M481 | core | 65.27 | 22.12 | 0.17 | 2.85 | 9.79 | 0.94 | 101.1 | 13.1 | 5.2 | 81.7 |

gm, groundmass

Glass. Many lavas have variably fresh brown to dark-brown interstitial glass (47 analyses). The observed compositions range from basaltic andesite to rhyolite, according to their classification utilizing the T.A.S. diagram (fig. 2; Table 6). A few glass compositions found in the basalt MAD10 (high La/Yb type) plot close to the trachyte-rhyolite boundary line (Fig. 2).

Accessories. The most important accessory phases of the evolved samples are cordierite, zircon, biotite and titanite. Cordierite (9 analyses) has been found in the Mailaka peraluminous rhyodacites; this phase has a narrow chemical range (Mg#=42-40; Melluso *et al.*, 2001). Biotite has been found as a rare phase in the Antampombato syenites, as are zircon and titanite.

## DISCUSSION

It is well known that most continental flood basalt provinces often have strongly different magma types (e.g., Peate, 1997), so that the search for a unique source or a single liquid line of descent is almost meaningless. Nevertheless, the study of the mineral and glass compositions offers an excellent opportunity to better identify different magma types and serial affinities, their crystallization histories, often in a single sample, and in fortunate cases also permits large-range correlations. At the same time, it is possible to exclude a common feeding system for samples showing similar chemical affinity, but located in different areas of the province. This is shown to be significant in distinguishing the transitional basalts of Mailaka with chemically and isotopically similar rock types exposed in the Antampombato dyke swarm and in the eastern coast of Madagascar.

### Whole-rock equilibration temperatures

The liquidus temperatures of the whole rocks, calculated utilizing algorithms obtained on anhydrous compositions (e.g., Eggins, 1993; Toplis and Carroll, 1995, 1996) give ranges from ca. 1300°C to ca. 1040°C from picritic basalts to evolved rocks (rhyodacites). The temperature of equilibration of the anhydrous pseudo-invariant point between olivine, plagioclase, clinopyroxene, low-Ca pyroxene and liquid (Grove and Juster, 1989), that has to be lower than in rocks with only olivine and/or plagioclase phenocrysts, never reached 1200 °C even in the most Mg-rich tholeiitic samples (the complete range is from 1184 to 1071 °C), and is in good agreement with
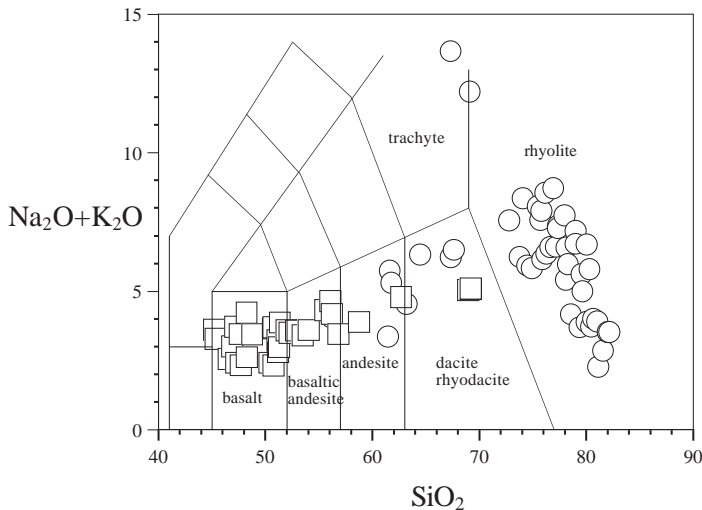


Fig. 2 – Total alkali silica diagram (T.A.S.; Le Bas *et al.*, 1986) with chemical composition of the Madagascan volcanic rocks considered in this paper (squares) and with glass composition in the mesostasis of lava flows (circles).
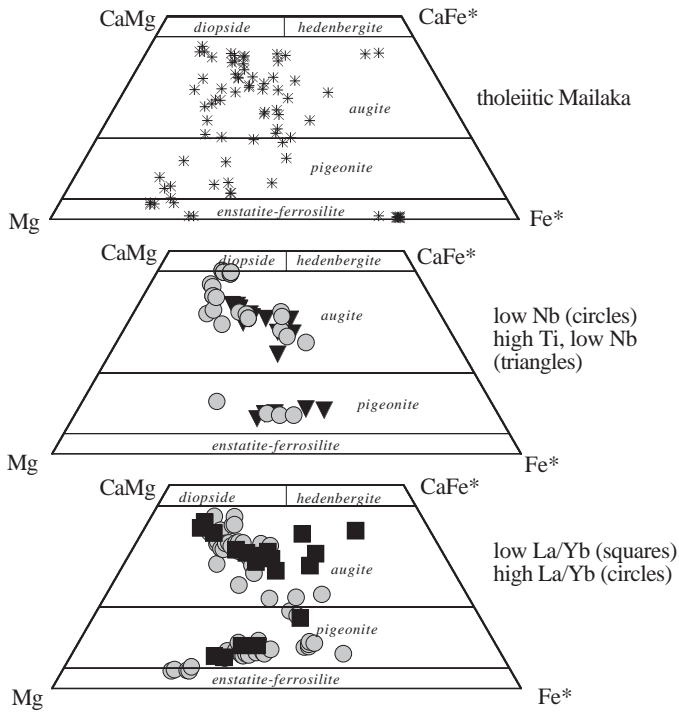
Fig. 3a – Compositional ranges of the pyroxenes of the tholeiitic rocks of the Madagascan province.
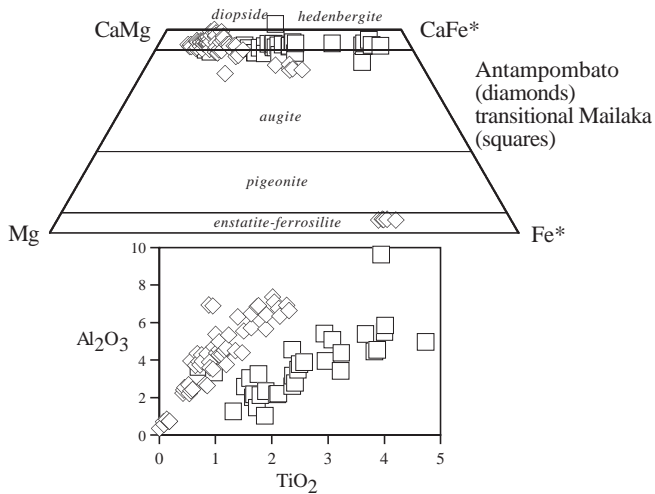


Fig. 3b – Compositional ranges of the pyroxenes of the transitional to alkaline rocks of Mailaka and Antampombato, and $TiO_2$-$Al_2O_3$ diagram for the same clinopyroxenes.

Fig. 4 – Compositional range of the Cr-bearing spinels of Madagascar.



Fig. 5 – Temperature-logfO$_2$ diagram for magnetite-ilmenite equilibrium pairs found in the Madagascan rocks. Symbols: squares, Antampombato; circles: high and low La/Yb eastern Madagascar; triangles: Mailaka basalts. MH, magnetite-hematite buffer, QFM, quartz-fayalite-magnetite buffer, NNO, nickel-nickel oxide buffer; WM, wüstite-magnetite buffer.

TABLE 5 – *Representative compositions of oxides. Ulvöspinel and ilmenite contents are reported in mole fractions. Cr#=Cr/(Cr+Al), Mg#=Mg/(Mg+Fe$^{2+}$).*

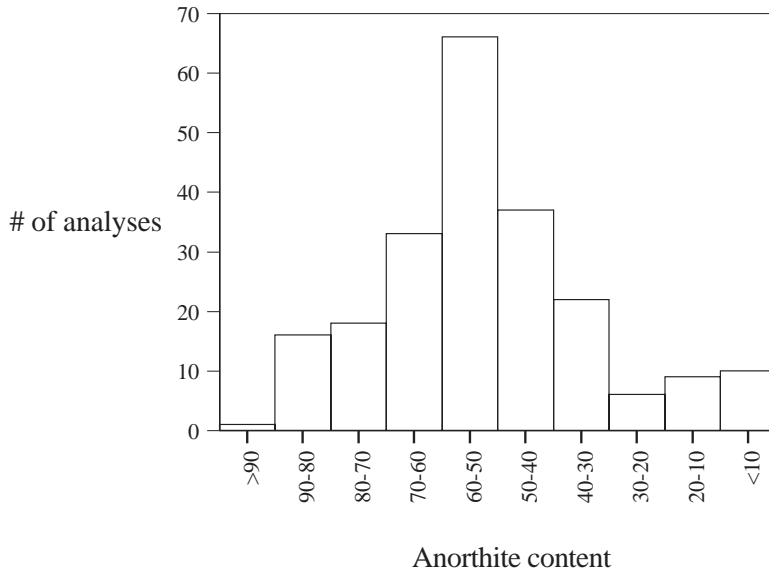| sample | | TiO$_2$ | Al$_2$O$_3$ | FeO | MnO | MgO | Cr$_2$O$_3$ | sum | Ulv | Cr | Ti+Fe''' | Al | Mg# | Cr# |
|---|---|---|---|---|---|---|---|---|---|---|---|---|---|---|
| M162 | core | 0.90 | 27.91 | 27.20 | 0.23 | 10.46 | 31.40 | 98.1 | 0.021 | 38.4 | 10.7 | 50.9 | 0.47 | 0.43 |
| M115 | core | 19.90 | 3.36 | 60.75 | 0.52 | 1.36 | 10.12 | 96.0 | 0.560 | 15.0 | 77.6 | 7.4 | 0.05 | 0.67 |
| M115 | gm | 25.71 | 2.07 | 68.01 | 0.63 | 0.95 | | 97.4 | 0.720 | 0.0 | 95.5 | 4.5 | 0.03 | |
| M158 | core | 17.00 | 5.05 | 57.09 | 0.49 | 1.25 | 16.31 | 97.2 | 0.470 | 23.7 | 65.4 | 10.9 | 0.05 | 0.68 |
| M158 | core | 1.02 | 37.80 | 26.88 | 0.43 | 14.00 | 18.14 | 98.3 | 0.022 | 20.8 | 14.5 | 64.6 | 0.59 | 0.24 |
| M129 | gm | 29.96 | 0.51 | 62.12 | 0.57 | 2.74 | | 95.9 | 0.849 | 0.0 | 98.9 | 1.1 | 0.08 | |
| M54 | gm | 26.19 | 1.25 | 67.21 | 0.44 | 0.84 | | 95.9 | 0.748 | 0.0 | 97.2 | 2.8 | 0.03 | |
| M7a | gm | 23.04 | 1.29 | 68.99 | 0.58 | 1.08 | | 95.0 | 0.661 | 0.0 | 97.1 | 2.9 | 0.04 | |
| M461 | core | 1.73 | 19.48 | 31.37 | 0.34 | 10.09 | 36.84 | 99.8 | 0.041 | 46.0 | 17.7 | 36.3 | 0.46 | 0.56 |
| M497 | core | 1.02 | 10.43 | 43.48 | 0.53 | 4.37 | 37.53 | 97.3 | 0.027 | 51.7 | 26.9 | 21.4 | 0.22 | 0.71 |
| M476 | gm | 26.76 | 0.14 | 69.00 | 4.29 | 0.10 | 0.02 | 100.3 | 0.738 | 0.0 | 99.7 | 0.3 | 0.00 | 0.11 |
| | | | | | | | | | ilm | | | | | |
| M146 | gm | 51.75 | 0.11 | 46.45 | 0.51 | 0.82 | | 99.6 | 0.978 | | | | | |
| M422 | gm | 55.04 | 0.01 | 33.40 | 1.43 | 8.09 | 0.44 | 98.4 | 0.998 | | | | | |
| M71 | gm | 48.58 | 0.30 | 46.52 | 0.40 | 2.65 | | 98.5 | 0.912 | | | | | |
| M6 | gm | 49.88 | 0.11 | 46.11 | 0.47 | 1.49 | | 98.1 | 0.952 | | | | | |
| M7a | gm | 49.76 | 0.15 | 46.27 | 0.54 | 1.42 | | 98.1 | 0.949 | | | | | |
| SM | gm | 50.48 | 0.12 | 48.06 | 0.71 | 0.35 | | 99.7 | 0.956 | | | | | |
| M484 | gm | 51.38 | | 42.78 | 5.25 | 0.03 | | 99.4 | 0.979 | | | | | |

gm, groundmass

Fig. 6 – Frequency histogram of plagioclase compositions (anorthite mol%) of Madagascan rocks.

TABLE 6 – *Average compositions (wt.% oxides) and one sigma standard deviation of glass found in the mesostasis of various samples.*

| sample | | $SiO_2$ | $TiO_2$ | $Al_2O_3$ | FeO | MnO | MgO | CaO | $Na_2O$ | $K_2O$ |
|--------|------|-------|-------|-------|-------|------|------|------|------|------|
| M153 | av | 78.26 | 1.08 | 11.54 | 2.28 | 0.07 | 0.05 | 0.84 | 2.64 | 3.23 |
|      | σ  | 0.97 | 0.12 | 0.23 | 0.60 | 0.06 | 0.03 | 0.19 | 0.60 | 0.13 |
| M160 | av | 74.27 | 0.89 | 12.56 | 3.92 | 0.08 | 0.23 | 1.33 | 2.87 | 3.85 |
|      | σ  | 1.47 | 0.21 | 0.56 | 0.23 | 0.05 | 0.15 | 0.82 | 0.46 | 0.18 |
| M19 | av | 62.48 | 1.12 | 12.26 | 13.10 | 0.14 | 1.18 | 4.80 | 3.17 | 1.76 |
|      | σ  | 0.71 | 0.02 | 1.42 | 0.98 | 0.00 | 0.47 | 0.34 | 0.90 | 0.51 |
| M7a | av | 78.81 | 0.78 | 11.30 | 1.10 | 0.10 | 0.05 | 0.64 | 2.46 | 4.77 |
|      | σ  | 1.42 | 0.11 | 0.65 | 0.31 | 0.05 | 0.07 | 0.83 | 0.51 | 0.59 |
| M10 | av | 68.21 | 0.78 | 16.16 | 1.72 | 0.05 | 0.03 | 0.12 | 4.41 | 8.52 |
|      | σ  | 0.90 | 0.48 | 1.51 | 0.85 | 0.04 | 0.02 | 0.01 | 0.56 | 0.17 |
| M40 | av | 76.43 | 0.56 | 13.40 | 1.10 | 0.03 | 0.03 | 0.61 | 4.01 | 3.84 |
|      | σ  | 1.30 | 0.19 | 0.94 | 0.30 | 0.03 | 0.04 | 0.13 | 0.71 | 0.74 |
| M6 | av | 80.95 | 0.85 | 12.14 | 1.77 | 0.02 | 0.13 | 0.49 | 0.98 | 2.68 |
|      | σ  | 0.67 | 0.10 | 0.73 | 0.22 | 0.03 | 0.13 | 0.25 | 0.06 | 0.33 |
| M74 | av | 65.26 | 1.96 | 12.78 | 9.94 | 0.12 | 0.39 | 3.36 | 4.63 | 1.56 |
|      | σ  | 2.44 | 0.45 | 0.77 | 2.37 | 0.05 | 0.15 | 0.81 | 0.14 | 0.17 |
| M54 | av | 77.42 | 0.94 | 11.79 | 2.71 | 0.07 | 0.02 | 0.40 | 3.02 | 3.62 |
|      | σ  | 0.66 | 0.17 | 0.27 | 0.13 | 0.08 | 0.02 | 0.26 | 0.83 | 0.27 |

the crystallization temperatures of the most Mg-rich pigeonites (up to 1173 °C) (fig. 7).

*Magma and within-sample evolution trends*

The frequent presence of fresh glass in the mesostasis of many samples provides an useful insight to the low-pressure magma evolution processes occurring in the Madagascan basalts. For this reason, fractionation models based on mass balance calculations between whole-rocks and matrix glass, using coexisting minerals as subtracted solids, have been performed for several lithotypes. The results (summarized in Table 7) indicate that, after substantial fractionation (70-90%) of plagioclase-bearing assemblages (34-50%
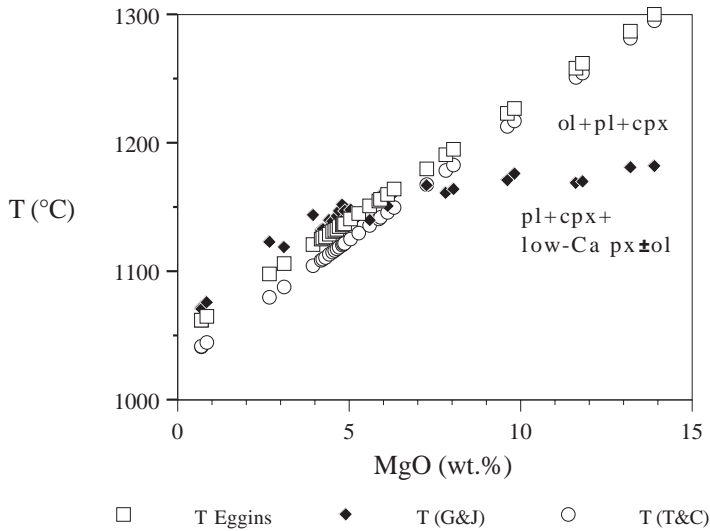


Fig. 7 – MgO-temperature relationships in the Madagascan samples obtained with three different geothermometers (see text and Table 1). The systematic lower temperature range obtained with the Grove and Juster geothermometer at relatively high MgO is clear indication that higher temperature phases (olivine± plagioclase± clinopyroxene) crystallized earlier than low-Ca pyroxenes, which became liquidus phases at lower temperatures (hence, at lower MgO content).

TABLE 7 – *Results of mass balance calculations between whole-rocks and the coexisting residual glass. $\sum R^2$=sum of the squared residuals; f=residual liquid fraction %.*

| from | | to | | ol | pl | cpx | opx/pig | sp | ilm | % sol | f | $\sum R^2$ |
|------|----|------|------|-----|------|------|---------|------|------|-------|------|------|
| M108 | BA | glass | rhy | | 46.7 | 41.2 | 5.0 | 7.1 | | 68.9 | 31.1 | 0.81 |
| M74 | BA | glass | rhy | | 41.9 | 32.5 | 10.8 | 14.8 | | 57.0 | 43.0 | 0.35 |
| M47 | bas | glass | rhy | 4.3 | 42.1 | 41.2 | | 12.4 | | 79.0 | 21.0 | 0.23 |
| M71 | bas | glass | and | | 44.9 | 31.2 | 15.2 | 8.7 | | 69.0 | 31.0 | 0.44 |
| M40 | bas | glass | rhy | | 34.0 | 35.8 | 8.0 | 8.9 | 3.3 | 81.0 | 19.0 | 0.08 |
| M19 | bas | glass | rhy | | 50.1 | 38.1 | 2.6 | 2.0 | 7.2 | 82.0 | 18.0 | 0.22 |
| M7a | bas | glass | rhy | | 48.5 | 21.5 | 18.9 | 5.1 | 6.0 | 87.0 | 13.0 | 0.03 |
| M10 | BA | glass | trach | | 41.3 | 22.5 | 13.6 | 1.5 | 6.4 | 85.2 | 14.8 | 0.58 |

rhy, rhyolite; and, andesite; trach, trachyte
ol, olivine; pl, plagioclase; cpx, clinopyroxene; opx/pig, orthopyroxene or pigeonite; sp, spinel; ilm, ilmenite

of the total mass subtracted) with similar amount of pyroxenes (ab. 40-43%) and less abundant Fe-Ti oxides (up to 13%), with a subtracted solid resembling gabbro and ferrogabbro, it is possible to obtain residual felsic glass, simply reducing the liquid content in a low-pressure closed system. The total transition from mafic rocks to strongly evolved residual whole-rock compositions was modelled by Melluso *et al.* (2001) with ca. 84% fractionation, but coupled with small input (10%) of silica-rich melt derived from crustal contamination processes, thus in broad agreement with the results shown here.

*Regional significance of the data*

From the data shown in this paper, we can provide some regional inferences: Clinopyroxenes belonging to the diopside-hedenbergite series are found in transitional to slightly alkaline rocks of both sides of the province, but their differing minor element contents prevent any type of chemical correlation. Pigeonitic clinopyroxenes occur in tholeiitic rocks from both sides of the province, whereas magnesian orthopyroxene, followed by pigeonite, has been found in some of the most Ti-rich basaltic rocks, testifying that a more alkaline nature of the rocks bears no relationship with their $TiO_2$ contents. On the other hand, no clear distinction has been found in the $TiO_2$ content of the various augites of the tholeiitic samples. Augites do not reach very high-Fe compositions, differently from Fe-salites of transitional rocks. No major difference in oxygen fugacity has been found in the studied mafic and intermediate rocks, testifying normally oxidizing conditions in the crystallization environment of the Madagascan volcanics.

## Concluding remarks

The chemical characteristics of the phases observed in the northern Madagascar basalts give evidence of a large range of crystallization temperatures (~300°C), which are typical of anhydrous tholeiitic liquids. Some remarkable features are given here:

– the liquids with typical tholeiitic affinity crystallize Ca-rich clinopyroxene of the augite-Fe-augite series, accompanied by low-Ca pyroxene (usually pigeonite);

– the liquids with transitional to alkaline affinity are in equilibrium with a clinopyroxene of the diopside-hedenbergite series, with a variable, though marked, Ti- and Al-enrichment in the intermediate terms (salites, Fe-salites); intrusive equivalents linked to these liquids can sporadically have also Ti-rich amphibole (kaersutite);

– olivine has a very large range of crystallization, from the most Mg-rich phenocryst cores to the extremely Fe-rich compositions in the groundmass. This large range is found in samples having olivine on the liquidus (i.e., mostly in the basalts); olivine reappears with a Fe-rich composition in strongly evolved rhyodacites, coexisting with orthopyroxene and cordierite;

– chromium-bearing spinels, found as inclusions in olivine of picritic basalts, basalts and in the dunitic rocks, have a wide compositional range, and include Al-rich, Cr-rich and Cr-bearing Fe-Ti-rich varieties, all of them crystallized from the most Mg-rich liquid compositions; magnetite-ulvöspinel solid solutions are poor in Cr and Al, and coexist with ilmenite in the late-crystallized mesostasis of basalts, basaltic andesites and andesites. They crystallized mostly at conditions close to the Quartz-Fayalite-Magnetite (QFM) oxygen buffer;

– the low content of $K_2O$ of the Madagascan magmas did not promote significant crystallization of K-bearing phases like alkali feldspar and biotite.

– the quartz-normative compositions of the glass fraction is strongly indicative of a residual liquid fraction after subtraction of the observed phenocryst compositions, giving further evidence of low-pressure evolution towards rhyolitic minimum melts in a broadly closed system.

The chemical variations given here are the basis for correlation between different magma types found in the southern part of the Madagascan province, and represent the background for trans-oceanic correlations between the coeval rocks found in southern India.

## REFERENCES

ANIL KUMAR G., PANDE K., VENKATESAN T.R. and BHASKAR RAO Y.J. (2001) – *The Karnataka Late Cretaceous dikes as products of the Marion hot spot at the Madagascar-India breakup event: evidence from $^{40}Ar/^{39}Ar$ geochronology and geochemistry*. Geophys. Res. Lett., **228**, 2715-2718.

BARDINTZEFF J.-M., BONIN B. and RASAMIMANANA G. (2001) – *The Cretaceous Morondava volcanic province (West Madagascar): mineralogical, petrological and geochemical aspects*. J. Afr. Earth Sci., **32**, 299-316.

DOSTAL J., DUPUY C., NICOLLET C. and CANTAGREL J.M. (1992) – *Geochemistry and petrogenesis of upper Cretaceous basaltic rocks from southern Madagascar*. Chem. Geol., **97**, 199-218.

LE BAS M.J., LE MAITRE R.W., STRECKEISEN A. and ZANETTIN P. (1986) – *A chemical classification of volcanic rocks based on the total alkali-silica diagram*. J. Petrol., **27**, 745-750.

EGGINS S.M. (1993) – *Origin and differentiation of picritic arc magmas, Ambae (Aoba), Vanuatu*. Contrib. Mineral. Petrol., **114**, 79-100.

GROVE T.L. and BRYAN W.B. (1983) – *Fractionation of pyroxene-phyric MORB at low pressure: an experimental study*. Contrib. Mineral. Petrol., **84**, 293-309.

GROVE T.L. and JUSTER T.C. (1989) – *Experimental investigations of low-Ca pyroxene stability and olivine-pyroxene-liquid equilibria at 1-atm in natural basaltic and andesitic liquids*. Contrib. Mineral. Petrol., **103**, 287-305.

ISHII T. (1976) – *The relations between temperature and composition of pigeonite in some lavas and their application to geothermometry*. Mineral. J., **8**, 48-57.

LE BAS M.J., LE MAITRE R.W., STRECKEISEN A. and ZANETTIN P. (1986) – *A chemical classification of volcanic rocks based on the total alkali-silica diagram*. J. Petrol., **27**, 745-750.

MELLUSO L., MORRA V., BROTZU P., RAZAFINIPARANY A., RATRIMO V. and RAZAFIMAHATRATRA D. (1997) – *Geochemistry and Sr-isotopic composition of the Cretaceous flood basalt sequence of northern Madagascar: petrogenetic and geodynamic implications*. J. Afr. Earth Sci., **24**, 371-390.

MELLUSO L., MORRA V., BROTZU P. and MAHONEY J.J. (2001) – *The Cretaceous igneous province of Madagascar: geochemistry and petrogenesis of lavas and dykes from the central-western sector*. J. Petrol., **42**, 1249-1278.

MELLUSO L., MORRA V., BROTZU P., D'ANTONIO M. and BENNIO L. (2002) – *Petrogenesis of the Late Cretaceous tholeiitic magmatism in the passive margins of northeastern Madagascar*. In: Menzies, M.A., Klemperer, S.L., Ebinger, C.J. and Baker J. (eds.): Volcanic Rifted Margins. Geol. Soc. Am. Spec. Paper, **362**, 83-98.

MELLUSO L., MORRA V., BROTZU P., FRANCIOSI L., PETTERUTI LIEBERCKNECHT A.M. and BENNIO L. (2003) – *Geochemical provinciality in the Cretaceous magmatism of northern Madagascar, and mantle source implications*. J. Geol. Soc. London, **160**, 477-488.

MELLUSO L., MORRA V., BROTZU P., TOMMASINI S., RENNA M.R., DUNCAN R.A., FRANCIOSI L. and D'AMELIO F. (2005) – *Geochronology and petrogenesis of the Cretaceous Antampombato-Ambatovy complex and associated dyke swarm, Madagascar*. J. Petrol., **46**, 1963-1996.

NIMIS P. (1999) – *Clinopyroxene geobarometry of magmatic rocks. Part 2. Structural geobarometers for basic to acid, tholeiitic and mildly alkaline magmatic system*s. Contrib. Mineral. Petrol., **135**, 62-74.

PEATE D.W. (1997) – *The Paraná-Etendeka Province*. In: Mahoney, J.J. and Coffin, M.F., (eds.) Large Igneous Provinces: Continental, oceanic and planetary flood volcanism. Am. Geophys. Union, Monograph **100**, 217-245.

ROEDER P.L. and EMSLIE R.F. (1970) – *Olivine-liquid equilibrium*. Contrib. Mineral. Petrol., **29**, 275-289.

STOREY M., MAHONEY J.J. and SAUNDERS A.D. (1997) – *Cretaceous basalts in Madagascar and the transition between plume and continental lithosphere mantle sources*. In: Mahoney, J.J. and Coffin, M.F., (eds.) Large Igneous Provinces: Continental, oceanic and planetary flood volcanism. Am. Geophys. Union, Mon. **100**, 95-122.

STOREY M., MAHONEY J.J., SAUNDERS A.D., DUNCAN R.A., KELLEY S.P. and COFFIN M.F. (1995) – *Timing of hot spot-related vulcanism and the breakup of Madagascar and India*. Science, **267**, 852-855.

Toplis M.J. and Carroll M.R. (1995) – *An experimental study of the influence of oxygen fugacity on Fe-Ti oxide stability, phase relations, and mineral-melt equilibria in ferro-basaltic systems*. J. Petrol., **36**, 1137-1170.

Toplis M.J. and Carroll M.R. (1996) – *Differentiation of ferro-basaltic magmas under conditions open and closed to oxygen: implications for the Skaergaard intrusion and other natural systems*. J. Petrol. **37**, 837-858.

Appendix. Analytical techniques

Mineral analyses on the most representative samples of this study have been performed at CNR laboratory of Padova, utilizing a CAMECA Camebax electron microprobe equipped with four Wavelenght Dispersive (WDS) spectrometers and one Energy Dispersive (EDS) spectrometer, and using a CAMECA SX50 electron microprobe at CNR-C.S.Q.E.A., Rome, using mixed EDS-WDS procedures. Silicates and oxides were used as standards. The Kakanui augite was used as monitor of accuracy. The data were reduced utilizing the CAMECA's PAP correction method. Whole-rock chemical analyses have been performed with X-Ray fluorescence, Atomic absorption spectrophotometry and gravimetric methods at Napoli, using techniques already described elsewhere (e.g., Melluso *et al.*, 1997).